Effects of Heat Treatment and Design on Mechanical Responses of NiTi Endodontic Instruments: a Finite Element Analysis

Suzanny Cristina Soares Martins[a]* [iD] *, Jéssica Dornelas Silva[a], Ana Cecília Diniz Viana[b],*

Vicente Tadeu Lopes Buono[a] [iD] *, Leandro Arruda Santos[a]*

[a]*Universidade Federal de Minas Gerais, Escola de Engenharia, Departamento de Engenharia Metalúrgica e de Materiais, Belo Horizonte, MG, Brasil*
[b]*Universidade Federal de Minas Gerais, Faculdade de Odontologia, Departamento de Odontologia Restauradora, Belo Horizonte, MG, Brasil*

Heat treatments and geometries have a significant influence on the mechanical behavior of endodontic files. Finite element analyses were performed to verify the effects due to each of these parameters in NiTi files. Two designs and three NiTi atomic structures (resultant from different heat treatments) were selected for this study. The geometries of the ProTaper Next X1 and ProTaper Universal S2 files, and the structures of fully austenitic (conventional superelastic), austenite treated, and fully R-phased were used. The mechanical responses were evaluated under flexion and torsion loading conditions described by ISO 3630-1 specification. According to the results, the design of the X1 file exhibit higher flexibility in comparison to the S2 model. Under torsional loads, S2 showed higher stiffness. The structures of fully austenitic showed the least flexibility under flexion and the highest torsional stiffness. The stress levels reached for the austenitic condition were uppermost. The treated condition that resulted in a fully R-phase file usually presented a higher level of flexibility with lower stress levels, indicating a longer life in fatigue when compared to the other treatments.

Keywords: *NiTi endodontic files, heat treatment, cross-sectional design, finite element analysis, bending and torsional loads.*

1. Introduction

The use of NiTi alloys in endodontic instruments had an enormous impact on endodontic practice. These alloys exhibit greater flexibility when compared with stainless steel[1]. Also, NiTi alloy presents superior biocompatibility and corrosion resistance[2,3]. Despite the advantages of NiTi over stainless steels, NiTi endodontic files may exhibit unexpected fractures within the root canal[4]. During canal preparation, endodontic files are subject to mechanical flexion and torsion loading caused by the canal anatomy itself, which is curved and narrow[5]. Thus, the fracture of these instruments usually occurs by torsional overload or flexural fatigue. The torsional fracture occurs when the file gets locked into the canal, whilst the shaft continues to rotate. The flexural failure occurs due to the material's fatigue: the instrument rotates within a curved channel and experiences alternating traction/compression loads, resulting in fatigue[4,6-8].

Several types of research have been done to prevent the failure of NiTi files[9-13]. The main focus is to improve the mechanical properties under bending and torsion, which is the main loading conditions to which the instruments are subjected during use, and, consequently, to increase its resistance to fatigue[4]. Variations in NiTi endodontic files have been made by different heat treatment conditions, geometric

changes (modifying the cross-sectional shape, pitch length, taper), and manufacturing conditions[14-16]. All these factors affect the clinical performance of rotary instruments.

Design elements of files have been widely investigated and demonstrated that pitch, cross-section shape, and area directly affect the mechanical behavior and degree of stress of these instruments[17-22]. However, most of these studies compare files with different geometries but do not take into consideration the fact that the material's constitution and properties are also different. The occurrence of more than one variable makes it difficult to determine if the mechanical responses presented by the instruments are due solely to the geometry or to a combination of this variable with materials properties.

Different heat treatments aim to improve the properties of the NiTi alloy used for endodontic instruments[15,16,23,24]. Heat treating conventional superelastic NiTi, which is in the austenite phase with B2 structure type, may transform its structure into an intermediate R-phase, which is a type of martensite with rhombohedral structure[16,25]. R-phase heat treatments increase flexibility and resistance to cyclic fatigue in NiTi files[16]. The recent effort in this area is to develop files containing R-phase fully or coexisting with austenite (commercially named M-wire)[4]. Many studies experimentally compare treated files, M-wire or R-phase, with conventional superelastic ones[5,15,26-28]. However, there

---
*e-mail: suzannymartins@gmail.com

are geometric variations between the evaluated instruments that may influence the results.

Since treatments and geometries seem to play an essential role in the file's behavior, in the present study, it was investigated the effects of these both variables on the mechanical of a NiTi endodontic instrument using finite element analysis (FEA). FEA offers the advantage of analyzing individual variables and combinations of them, distinguishing the influences due to geometry or heat treatment. Two designs with significant differences in the shape and area of the cross-section and the distribution of mass along its axis (one being eccentric and the other concentric) were chosen, and three NiTi structures obtained by distinct heat treatment conditions were selected for this study. The geometries of the ProTaper Next X1 and ProTaper Universal S2 files were adopted. The following three structures were used: i) fully austenitic (conventional superelastic); ii) recovered austenite superelastic with rearranged dislocation due to the heat treatment that made the dislocations move, reorganize and annihilated each other resulting in a different structure; and iii) fully R-phased.

2. Materials and Methods

Two commercial files ProTaper Next X1 and ProTaper Universal S2 were chosen to analyze the variation in mechanical behavior due to geometry. Three conditions were used to investigate the effects of heat treatment on the behavior of the files: state as received, heat-treated at 350 °C, and heat-treated at 450 °C.

Three-dimensional models were created using computer-assisted design (CAD) software SolidWorks 2016 to reproduce the current geometries of the ProTaper Next X1 and

ProTaper Universal S2 files (Figures 1a and b, respectively). Both instruments have a similar diameter (0.17 mm and 0.20 mm tip diameter, for X1 and S2, respectively) and the same taper (0.04). However, they exhibit differences in cross-sectional shape, as can be seen in Figure 1. Also, X1 showing an eccentric cross-section geometry and S2 being concentric. The instruments had an active part length of 17 mm and a total length of 25 mm.

The 3D models have been exported to Abaqus 6.14-2 software and meshed for the finite element analysis (FEA) with 20-noded quadratic elements C3D20R (see Figure 2). For the mesh generation, it aimed to maintain the same element size for both geometries. The element size was defined so that it was possible to apply the same loads for the three sets of properties in each geometry. The final finite element model of the X1 consisted of 2,244 elements with 13,329 nodes. The S2 model was composed of 2,292 elements integrating 13,038 nodes.

The heat treatment conditions applied, as well as the mechanical properties resulting from each condition, were obtained from work performed by Silva et al.[29], which heat-treated an initially superelastic NiTi wire in various temperatures. For this study, three conditions were chosen that resulted in more distinct properties and structures. The as-received (AR) condition and heat treatment conditions performed at 350 °C and 450 °C were selected. According to Silva et al.[29], the microstructure of AR condition is superelastic austenite, with a high density of dislocations and defects; the condition at 350 °C displays recovered superelastic austenite, with rearranged dislocations; and the condition at 450 °C is R-phase structure.
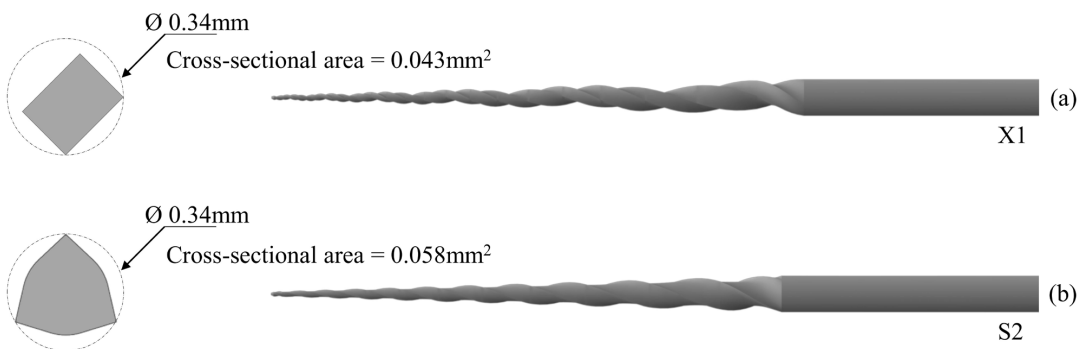

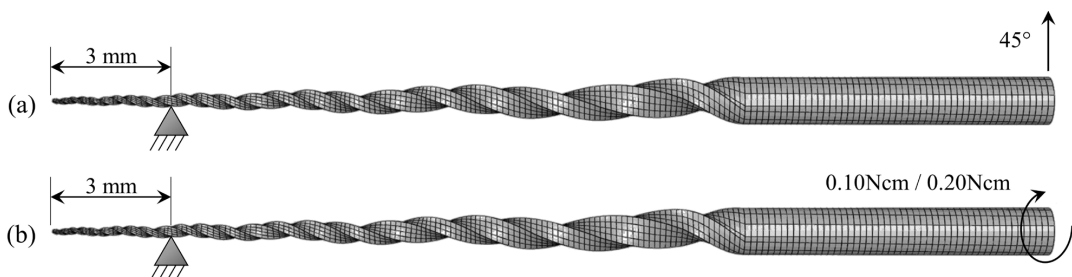**Figure 1.** Geometric model and cross-section at 3 mm from the tip of the analyzed files: (a) X1 and (b) S2.

Figure 2. Boundary conditions used for (a) the bending and (b) torsion test, based on ISO 3630-1[31].

The samples will be named by combining the geometry with the heat treatment according to the examples: X1_350 is the X1 file with the treatment conditions at 350 °C; S2_AR refers to the S2 geometry with the condition parameters as received.

The behavior of a superelastic alloy was simulated with the aid of a user-defined subroutine implemented in the Abaqus code based on the constitutive model proposed by Auricchio and Petrini[30]. The required parameters for this subroutine extracted from the work of Silva et al.[29] are described in Table 1.

Figure 2 shows the boundary conditions used in this study to reproduce experimental bending and torsion tests for endodontic instruments based on ISO 3630-1 specification[31]:

1) For the bending resistance test, the file was held at 3 mm from the tip, preventing any displacement in the x, y, and z axes. The shaft was then deflected until 45° of inclination;

2) For the torsion resistance test, the endodontic instrument was also held at 3 mm from the tip, and clockwise torsional moments of 0.10 Ncm for X1 and 0.20 Ncm for S2 were applied at the

end of the shaft. The different torsion values were chosen based on the mechanical resistance of the instruments under uniaxial tensile tests, so as not to reach their yield limit.

The mechanical behavior was characterized in terms of flexibility and stress distribution. The stresses in the file models were depicted in terms of von Mises equivalent stress.

3. Results

3.1 Bending tests

Figure 3 shows the variation of the simulated bending moment caused by the flexion of the files up to 45°. In this context, flexibility can be defined as the moment needed to bend the instrument without causing permanent deformation. X1 geometry provides greater flexibility than S2. In general, the heat treatment at 450 °C resulted in higher flexibility than the heat treatment at 350 °C. The AR condition is the least flexible.

A peculiarity is noted in X1_450 when compared with the other conditions. Initially, X1_450 exhibits greater flexibility,

Table 1. Parameters used to describe the constitutive model for simulation.

| Parameter	Description	AR	S350	S450
E_A	Austenite elasticity	55,737 MPa	42,389 MPa	52,192 MPa
V_A	Austenite Poisson's ration	0.33	0.33	0.33
E_M	Martensite elasticity	19,106 MPa	22,383 MPa	20,877 MPa
V_M	Martensite Poisson's ration	0.33	0.33	0.33
ε^L	Transformation strain	8.6%	7.2%	6.4%
$(\delta\sigma/\delta T)_L$	$(\delta\sigma/\delta T)$ loading	6.7	6.7	6.7
σ_L^S	Start of transformation loading	448 MPa	389 MPa	316 MPa
σ_L^E	End of transformation loading	511 MPa	459 MPa	355 MPa
T_0	Reference temperature	25 °C	25 °C	25 °C
$(\delta\sigma/\delta T)_U$	$(\delta\sigma/\delta T)$ unloading	6.7	6.7	6.7
σ_U^S	Start of transformation unloading	161 MPa	104 MPa	6.95 MPa
σ_U^E	End of transformation unloading	118 MPa	43 MPa	6.95 MPa
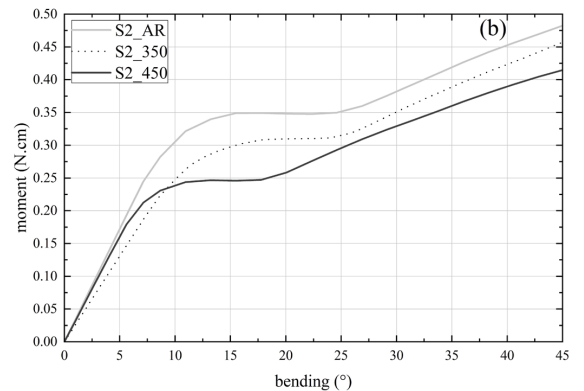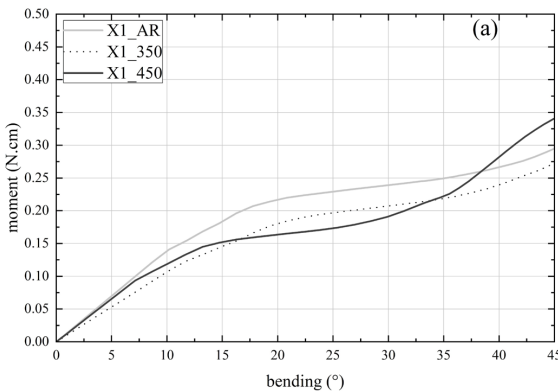
Figure 3. Numerical moment-bending curves: (a) X1 file and their respective heat treatment conditions and (b) S2 file and their respective heat treatment conditions.

but around 33° of bending its behavior changes, reaching the lowest flexibility at 45°. This behavior occurs due to the shorter length of the martensitic transformation plateau verified for the condition treated at 450 °C (see Table 1). At 45°, the elastic deformation of martensite already occurs for X1_450, in which there is a greater inclination due to the stress rising at a higher rate.

A maximum moment of 0.295 Ncm was calculated for X1_AR. For X1_350 and X1_450 the maximum moments were 0.273 Ncm and 0.341 Ncm, respectively. S2_AR exhibited 0.483 Ncm at 45°, for S2_350 it was 0.457 Ncm and for S2_450, 0.412 Ncm.

The von Mises stress distributions along with the instruments and in the cross-section at 3 mm from the tip under bending are illustrated in Figures 4 and 5, respectively. The von Mises stress for S2 design is higher than the one

calculated for X1: S2 reaches values close to 1,400 MPa, while X1 does not exceed 1,000 MPa. Both heat treatments decreased the stress level, being the treatment at 450 °C the most effective in terms of stress reduction under bending, which means the ideal condition to obtain more flexible instruments. The highest von Mises stresses were obtained in AR condition. The stress is concentrated near the tip held region and located at the periphery of the cross-section, whereas the central area exhibited zero or lower stresses.

Figure 6 shows the mean stress curves in the cross-sections illustrated in Figure 5. The stresses achieved for X1 are lower than the ones calculated for S2, considering the same condition. The improvement in bending resistance at 450 °C is observed for both geometries. Again, the heat treatment at 450 °C generated the lowest stress levels, while AR reached the highest stress.
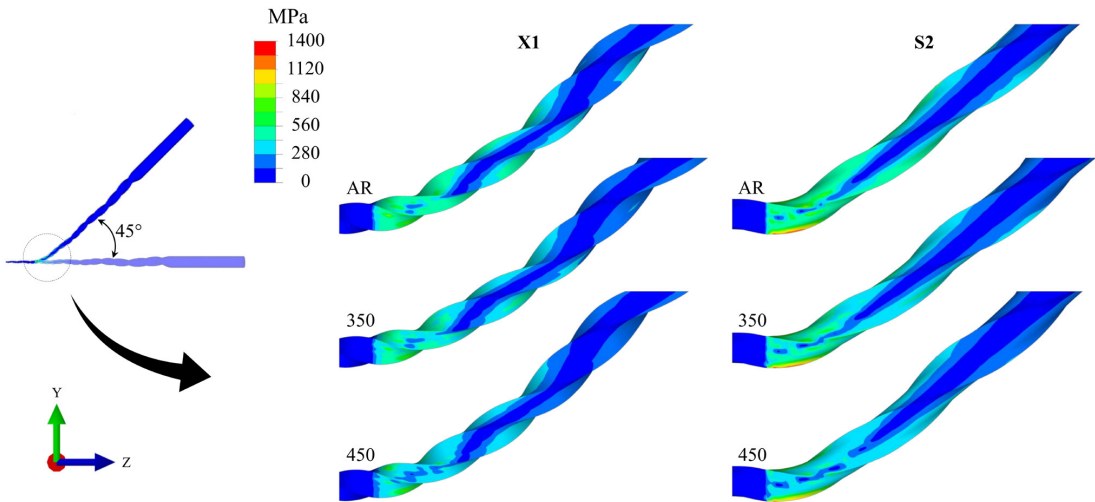

Figure 4. The von Mises stress distribution along with the body instruments under bending at 45°.
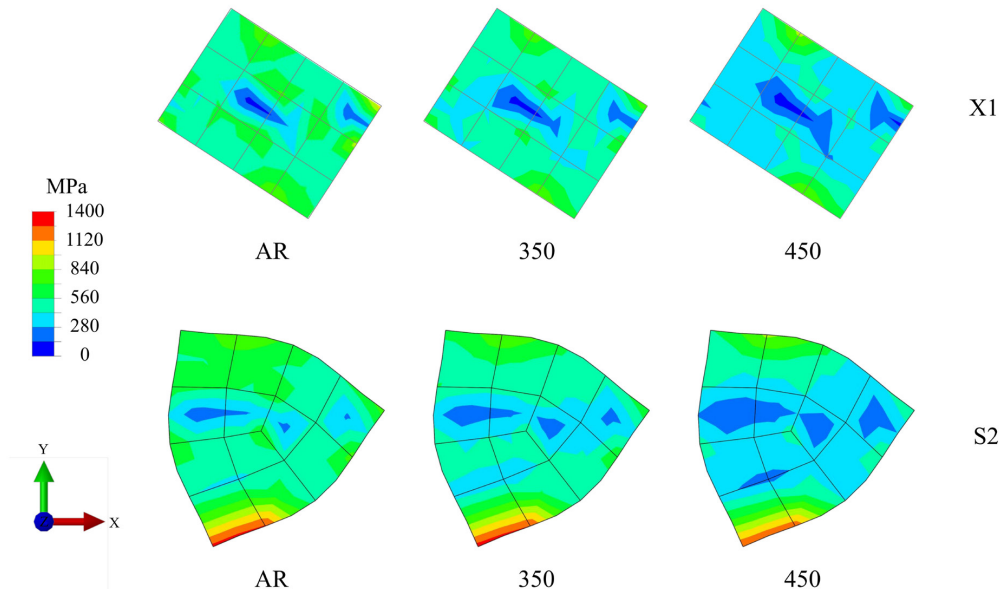

Figure 5. The von Mises stress distribution in the cross-section at 3 mm from the tip under bending at 45°. Note that the neutral lines are set in the x direction, which means that the flexural displacement was applied in the y direction.

3.2 Torsion test

Figure 7 shows the distortion angles as a function of the applied torque under torsional loading. The curves are interrupted at the maximum torsional moment used of 0.10 Ncm for X1, and 0.20 Ncm for S2. Considering the torsional stiffness as the moment needed to rotate the instrument, it is observed that the S2 files are more rigid than the X1 ones. For both geometries, the heat treatments resulted in similar behavior. The AR condition presented the superior stiffness, whilst the heat treatment at 450 °C reduced the torsional stiffness of the instruments. The total angular displacement for X1_AR, X1_350, and X1_450 was 63.0°, 82.1°, and 109.3°, respectively. The S2_AR presented an angular displacement of 88.1°, S2_350 present 97.4°, and S2_450 deformed up to 117.9°.

Figures 8 and 9 illustrated the von Mises stress distribution in the files after the torsion resistance test along with the body and the cross-section, respectively. To facilitate data analysis, the stresses shown under torsion are presented considering the maximum torsional moment of 0.10 Ncm for both geometries in all conditions.

The stress is concentrated near the constrained part and decreased as it moved away from the tip. The highest stresses were located at the periphery of the cross-section. Unlike what happens under bending, the high stresses are located in central regions, between the cutting edges, and not at the corners. Also, certain symmetry is verified in the stress distribution under twisting.

In X1 geometry, the heat treatments increased the stress on the surfaces of the files and, at the same time, diminished the stress in the central area. The opposite happens for S2, with stress reduction in peripheral regions, while the central part presented a slight decrease in stress.

The average stress curve under torsion up to 0.10 Ncm for both geometries in all conditions is exhibited in Figure 10. It is noted that the stress levels achieved in S2 are considerably lower than in X1. When applying the same torque to both instruments, S2 deforms less, resulting in lower stresses. Concerning heat treatment, results were similar to the ones under the bending condition, where heat treatment at 450 °C promoted the most moderate stresses considering the same angle.

4. Discussion

NiTi alloys were applied to endodontic instruments to facilitate the process of shaping root canals. However, unexpected fractures may occur in these files. Manufacturers seek to eliminate this problem by exploring several areas, including geometric changes, heat treatments, and manufacturing processes[32,33].
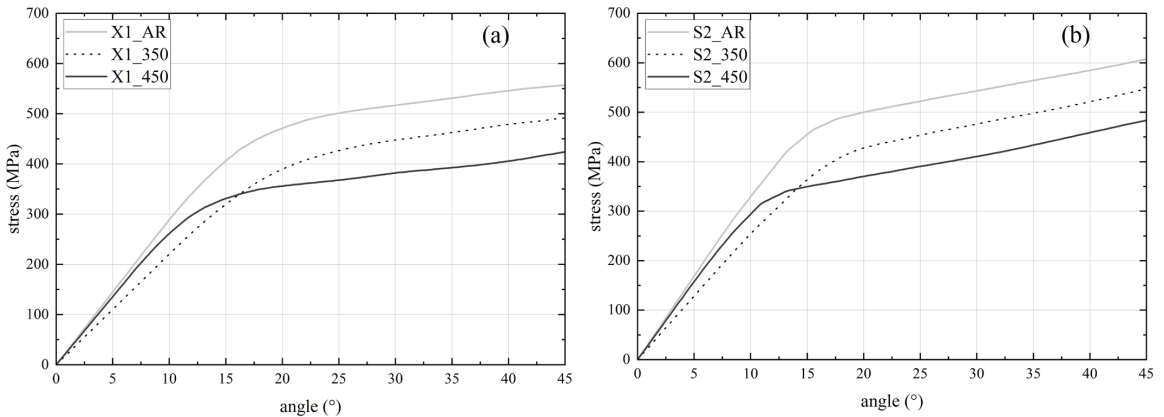

Figure 6. Mean stress curves under bending until 45°: (a) X1 file and their respective heat treatment conditions and (b) S2 file and their respective heat treatment conditions.
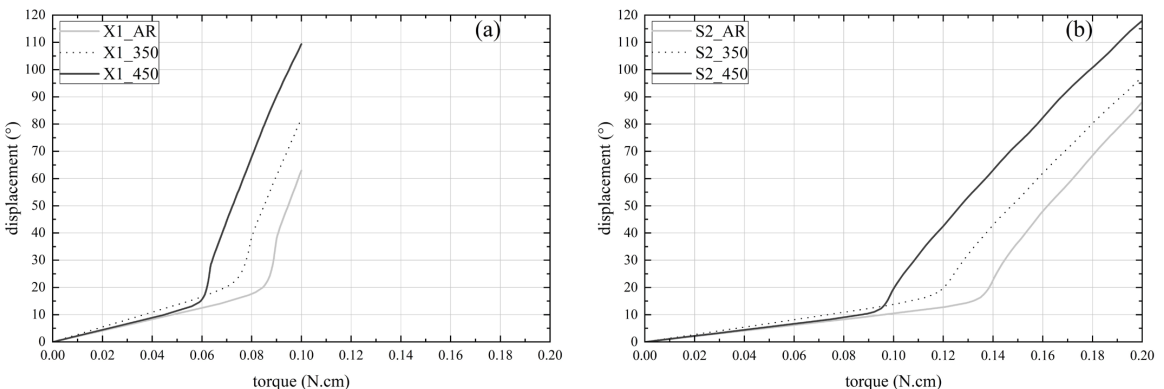

Figure 7. Numerical displacement-torque curves: (a) X1 file and their respective heat treatment conditions and (b) S2 file and their respective heat treatment conditions.
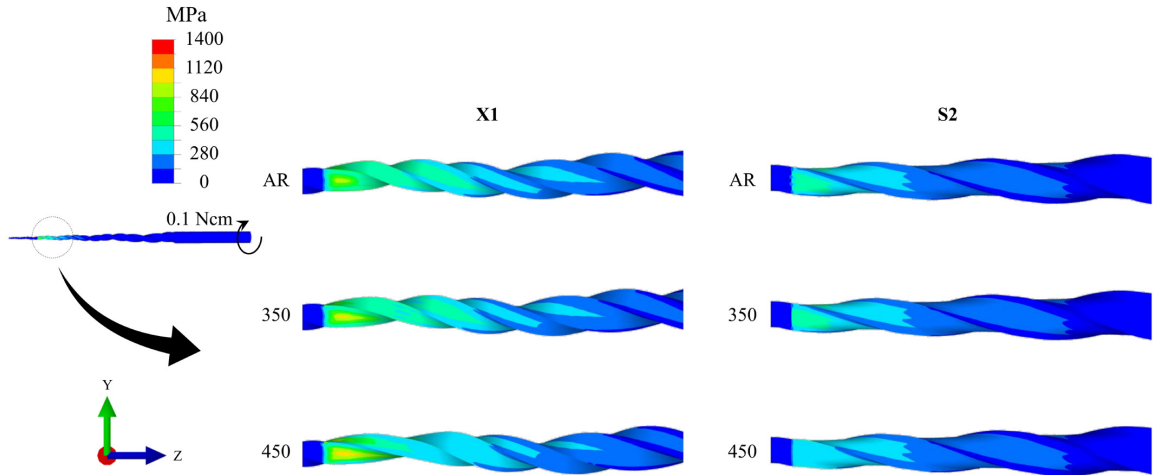
Figure 8. The von Mises stress distribution along with the body instruments under torsion at 0.10 Ncm clockwise.
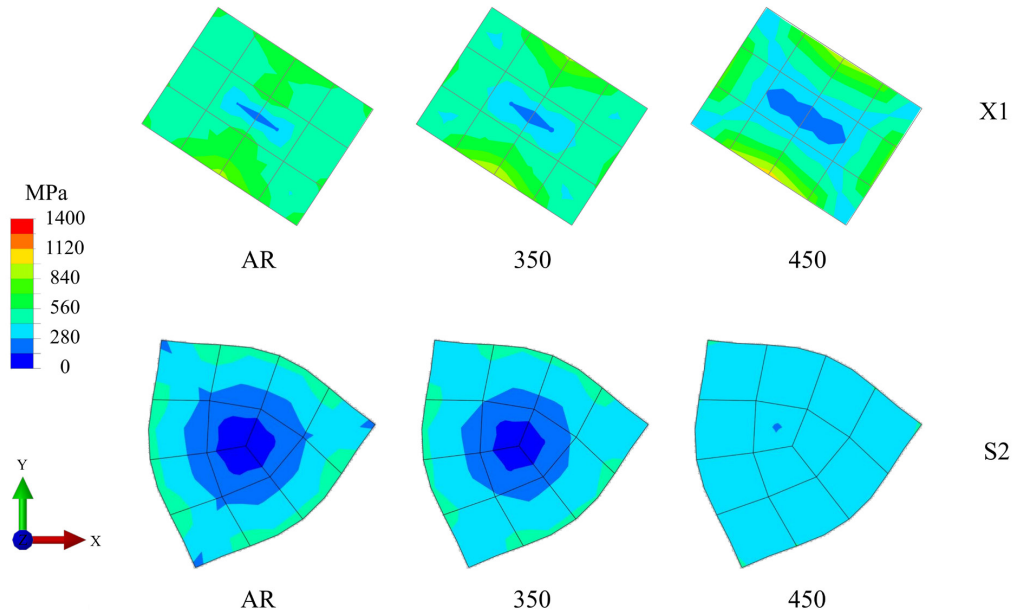

Figure 9. The von Mises stress distribution in the cross-section at 3 mm from the tip under torsion at 0.10 Ncm clockwise.
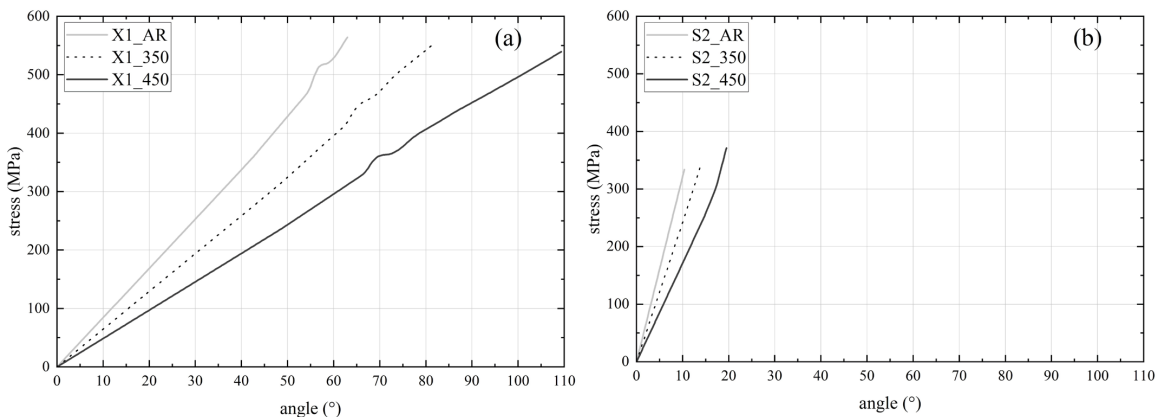

Figure 10. Mean stress curves under torsion up to 0.10 Ncm: (a) X1 file and their respective heat treatment conditions and (b) S2 file and their respective heat treatment conditions.

Several changes in design have been made to the shape of the cross-section, in its eccentricity, taper and pitch[34,35]. Heat treatments have also been widely applied to improve the fatigue resistance of endodontic instruments. The thermal process carried out in conventional NiTi alloys alter the atomic structures present in this material and, consequently, modify its mechanical properties[33,36]. NiTi alloys can have three phases in their microstructure: austenite, martensite, and R-phase. The austenite phase is resistant and rigid, while martensite and R-phase are flexible and quite ductile. The compositions of the three phases have an enormous influence on the mechanical characteristics of NiTi, and the presence of these phases is directly related to the heat treatment[25,33]. Depending on the heat treatment performed, the martensitic transformation can happen in a single stage (austenite (A) to martensite (M)) or two stages (A to R to M). Generally, the single-stage occurs in Ni-rich NiTi alloys, and the dual-stage transformation happens after a previous treatment that results in fine and dispersed Ni_3Ti_4 precipitates in the austenitic matrix[36].

With so many possible variations to be made on endodontic files, manufacturers already explored a myriad of production routes to achieve better clinical behavior. However, at research levels, it is not precisely known what the influence is due to each variation in an isolated way since commercial files differ from both geometry and material frequently. Thus, the present work sought to link each response of the files to their mechanical/metallurgical alteration. For this, using the finite element method, two different file geometries were compared, applying three conditions of heat treatment of NiTi alloys. The behavior of these files was analyzed by bending and torsion test.

Numerical results of the mechanical behavior showed that the X1 geometry promotes greater flexibility under flexion and less torsional stiffness to the instrument when compared to S2. This fact is intrinsically related to the cross-section of each file. Higher torsional stiffness in S2 was already expected since the area of its cross-section is 35% larger than that of X1 (Figure 1). Several studies reported that larger cross-sectional areas have a higher torsional stiffness[34,35,37]. The resistance to torsion is required to maintain the cutting edge geometry and maintain your efficiency[15,38].

For design X1, the torsional stiffness is lower, but its flexibility under bending is higher than S2. In general, greater flexibility means lower torsional stiffness in cases of smaller cross-section[4,39,40]. This behavior can be confirmed by Figures 3 and 7. High flexibility is required because this allows rotary instruments to follow the curvature of the root canal more efficiently, keep its original shape[1,7,15]. The flexibility in X1 can be related both to its smaller cross-sectional area and to the instrument's eccentricity. First, the flexibility was inversely proportional to the area moment of inertia. Also, the eccentric geometry of the cross-section modifies the mass distribution along the axis of the instrument. Due to this off-centered geometry, some studies that compared concentric and eccentric files found that off-centered files had greater flexibility, just like it was verified here[22,27,41-43]. However, there are other variables present in these studies that can simultaneously affect flexibility, such as the shape and area of the cross-section, pitch, and taper, as in the present study.

As shown in Figures 4-6 and Figures 8-10, the geometric differences between X1 and S2 change the stress level in the files. X1 experienced lower stress under bending than the S2. These results suggest that X1 instruments might experience a longer fatigue life. Since X1 is subjected to lower levels of stress, it would postpone its rupture by bending.

Under torsion, it was S2 who exhibited the lowest stress levels. This fact is associated with the higher torsional stiffness presented by S2. Because S2 is more resistant to torsion loading, it reaches much lower levels of stress, as seen in Figure 10.

Regarding thermal treatments, it was observed that the condition AR, which exhibits austenite in its structure, provides the least flexibility and, consequently, the highest torsional stiffness. Previous studies have already reported this fact[4,5,24]. With the heat treatment at 350 °C, the phase present in the material is still austenite, but with recovered and rearranged dislocations. This condition of heat treatment promoted an increase in flexibility when compared to AR. This behavior is related to the reduction of the start of transformation loading (Table 1), in which the material enters the region of the plateau with lower stress. As a consequence of the increase in flexibility, there is a decrease in torsional stiffness.

The heat treatment carried out at 450 °C promoted an even more significant structural change than at 350 °C. In this case, the austenitic matrix is replaced by the R-phase. This phase is more flexible than austenite, as seen for S2 geometry, and as some studies have reported[4,9,24,44,45]. Usually, the R-phase also promotes a considerable increase in flexibility of instruments due to its lowest elastic modulus and plateau stress values[4,9,24]. However, it is noteworthy that particular behavior was observed under flexion for the X1_450 file (Figure 3). It was found that, initially, the condition treated at 450 °C resulted in superior flexibility. However, by the end of the test, the bending behavior changes. A difference in inclination is observed after 35°, and X1_450 reached a moment value higher than X1_AR and X1_350 at 45°. This behavior is associated with the presence of the R-phase and the geometry of the instrument. As the R-phase is an intermediate phase between austenite and martensite, it is easier to transform R-phase into martensite. This facility is due to the lower level of transformation, both in terms of stress and percentage of strain. Thus, it appears that the X1_450 file is more flexible in smaller angular deflections. However, for higher deflections, X1 treated at 450 °C becomes less flexible than the other X1 conditions. It occurs because X1_450 reaches the end of the martensitic transformation faster than X1_350, and AR, that is, exhibits a smaller plateau. Thus, the X1_450 condition entering in the field of elastic deformation of martensite. As a result, the stress increases with a higher deflection rate, reaching a higher moment value. This atypical behavior is not observed for S2. It can be seen that the geometry of X1 changes the moment of transformation of the R-phase into martensite.

The lowest stress value was related to the condition treated at 450 °C. R-phase has a much smaller stiffness than the other phases. Because of that, this structure allows stress relaxation during the deformation of endodontic instruments. The stresses reached by a file are related to its useful life. The fatigue life varies inversely with the amplitude of the

stress to which the files are subjected in the shape canal procedure[46]. The instruments treated at 450 °C exhibited low-stress values under bending. This performance indicates that R-phase tends to be more fatigue resistant. Even under torsion, R-phase models show low stresses. It would mean a satisfactory performance against failure due to torsional overloading[4]. The analysis of the R-phase exhibiting a longer fatigue life is similar to the results obtained by Silva et al.[29]. Silva et al.[29] verified by experimental tests that the fatigue life of the three conditions used in the present work. The authors demonstrated that its samples treated at 450 °C have higher fatigue resistance than at 350 °C, which in turn is superior to AR. Therefore, the results obtained by simulation agree with the experimental data.

5. Conclusions

In this paper, the effects of treatments and geometries on endodontic files were studied. The following conclusions could be drawn:

- The design influences the mechanical behavior of endodontic files. Increased flexibility is achieved for a smaller cross-sectional area and with geometric eccentricity. The torsional stiffness is improved by increasing the cross-sectional area.
- Geometry changes the pattern of stress distribution, influencing the fatigue resistance of files. The eccentric file generated less stress than the concentric one.
- Heat treatments alter the phases present in the NiTi alloy by modifying its mechanical properties. R-phase usually offers greater flexibility and tends to be more resistant to fatigue than austenite.

6. Acknowledgments

7. References

1. Legrand V, Moyne S, Pino L, Arbab Chirani S, Calloch S, Chevalier V, et al. Mechanical behavior of a NiTi endodontic file during insertion in an anatomic root canal using numerical simulations. J Mater Eng Perform. 2015;24(12):4941-7. http://dx.doi.org/10.1007/s11665-015-1799-0.

2. Gavini G, Santos M, Caldeira CL, Machado MEL, Freire LG, Iglecias EF, et al. Nickel-titanium instruments in endodontics: a concise review of the state of the art. Braz Oral Res. 2018;32(suppl 1):44-65. http://dx.doi.org/10.1590/1807-3107bor-2018.vol32.0067. PMid:30365608.

3. Carmine M, Fabrizio N, Emanuele S, Franco F. Analysis of fatigue damage in shape memory alloys by nanoindentation. Mater Sci Eng A. 2017;684:335-43. http://dx.doi.org/10.1016/j.msea.2016.12.003.

4. Santos LDA, Resende PD, Bahia MGDA, Buono VT. Effects of R-Phase on mechanical responses of a nickel-titanium

5. endodontic instrument: structural characterization and finite element analysis. ScientificWorldJournal. 2016;2016:1-11. http://dx.doi.org/10.1155/2016/9273078. PMid:27314059.

5. Galal M, Ismail AG, Omar N, Zaazou M, Nassar MA. Influence of thermomechanical treatment on the mechanical behavior of protaper gold versus protaper universal (a finite element study). Open Access Maced J Med Sci. 2019;7(13):2157-61. http://dx.doi.org/10.3889/oamjms.2019.552. PMid:31456845.

6. Arruda Santos L, López JB, de Las Casas EB, Azevedo Bahia MG, Buono VT. Mechanical behavior of three nickel-titanium rotary files: a comparison of numerical simulation with bending and torsion tests. Mater Sci Eng C. 2014;37:258-63. http://dx.doi.org/10.1016/j.msec.2014.01.025. PMid:24582247.

7. Montalvão D, Shengwen Q, Freitas M. A study on the influence of Ni-Ti M-Wire in the flexural fatigue life of endodontic rotary files by using Finite Element Analysis. Mater Sci Eng C. 2014;40:172-9. http://dx.doi.org/10.1016/j.msec.2014.03.061. PMid:24857480.

8. Shim K, Oh S, Kum K, Kim YC, Jee KK, Chang SW. Mechanical and metallurgical properties of various nickel-titanium rotary instruments. BioMed Res Int. 2017;2017:1-13. http://dx.doi.org/10.1155/2017/4528601. PMid:29318149.

9. Braz Fernandes FM, Alves AR, Machado A, Oliveira JP. Effect of heat treatments on Ni-Ti endodontic files. Cienc e Tecnol dos Mater. 2017;29(1):e15-8.

10. Lo Savio F, Pedullà E, Rapisarda E, La Rosa G. Influence of heat-treatment on torsional resistance to fracture of nickel-titanium endodontic instruments. Procedia Struct Integr. 2016;2:1311-8. http://dx.doi.org/10.1016/j.prostr.2016.06.167.

11. Gambarini G, Grande NM, Plotino G, Somma F, Garala M, De Luca M, et al. Fatigue resistance of engine-driven rotary nickel-titanium instruments produced by new manufacturing methods. J Endod. 2008;34(8):1003-5. http://dx.doi.org/10.1016/j.joen.2008.05.007. PMid:18634935.

12. Larsen CM, Watanabe I, Glickman GN, He J. Cyclic fatigue analysis of a new generation of nickel titanium rotary instruments. J Endod. 2009;35(3):401-3. http://dx.doi.org/10.1016/j.joen.2008.12.010. PMid:19249604.

13. Versluis A, Kim H, Lee W, Kim BM, Lee CJ. Flexural stiffness and stresses in nickel-titanium rotary files for various pitch and cross-sectional geometries. J Endod. 2012;38(10):1399-403. http://dx.doi.org/10.1016/j.joen.2012.06.008. PMid:22980187.

14. Melo MCC, Pereira ESJ, Viana ACD, Fonseca AM, Buono VT, Bahia MG. Dimensional characterization and mechanical behaviour of K3 rotary instruments. Int Endod J. 2008;41(4):329-38. http://dx.doi.org/10.1111/j.1365-2591.2007.01368.x. PMid:18217988.

15. Prados-Privado M, Rojo R, Ivorra C, Prados-Frutos JC. Finite element analysis comparing WaveOne, WaveOne Gold, Reciproc and Reciproc Blue responses with bending and torsion tests. J Mech Behav Biomed Mater. 2019;90:165-72. http://dx.doi.org/10.1016/j.jmbbm.2018.10.016. PMid:30366307.

16. Gu Y, Kum KY, Perinpanayagam H, Kim C, Kum DJ, Lim SM, et al. Various heat-treated nickel–titanium rotary instruments evaluated in S-shaped simulated resin canals. J Dent Sci. 2017;12(1):14-20. http://dx.doi.org/10.1016/j.jds.2016.04.006. PMid:30895018.

17. Basheer Ahamed SB, Vanajassun PP, Rajkumar K, Mahalaxmi S. Comparative evaluation of stress distribution in experimentally designed nickel-titanium rotary files with varying cross sections: a finite element analysis. J Endod. 2018;44(4):654-8. http://dx.doi.org/10.1016/j.joen.2017.12.013. PMid:29426643.

18. Berutti E, Chiandussi G, Gaviglio I, Ibba A. Comparative analysis of torsional and bending stresses in two mathematical models of nickel-titanium rotary instruments: ProTaper versus ProFile. J Endod. 2003;29(1):15-9. http://dx.doi.org/10.1097/00004770-200301000-00005. PMid:12540212.

19. La Rosa G, Lo Savio F, Pedullà E, Rapisarda E. Developing of a new device for static and dynamic tests of Ni-Ti instruments for root canal treatment. Procedia Struct Integr. 2016;2:1303-10. http://dx.doi.org/10.1016/j.prostr.2016.06.166.

20. Turpin YL, Chagneau F, Vulcain JM. Impact of two theoretical cross-sections on torsional and bending stresses of nickel-titanium root canal instrument models. J Endod. 2000;26(7):414-7. http://dx.doi.org/10.1097/00004770-200007000-00009. PMid:11199768.

21. Ha J, Kim SK, Cohenca N, Kim HC. Effect of R-phase heat treatment on torsional resistance and cyclic fatigue fracture. J Endod. 2013;39(3):389-93. http://dx.doi.org/10.1016/j.joen.2012.11.028. PMid:23402513.

22. Ha JH, Kwak SW, Versluis A, Lee CJ, Park SH, Kim HC. The geometric effect of an off-centered cross-section on nickel–titanium rotary instruments: A finite element analysis study. J Dent Sci. 2017;12(2):173-8. http://dx.doi.org/10.1016/j.jds.2016.11.005. PMid:30895044.

23. Özyürek T, Uslu G, Yılmaz K, Gündoğar M. Effect of glide path creating on cyclic fatigue resistance of reciproc and reciproc blue nickel-titanium files: a laboratory study. J Endod. 2018;44(6):1033-7. http://dx.doi.org/10.1016/j.joen.2018.03.004. PMid:29680720.

24. Zupanc J, Vahdat-Pajouh N, Schäfer E. New thermomechanically treated NiTi alloys – a review. Int Endod J. 2018;51(10):1088-103. http://dx.doi.org/10.1111/iej.12924. PMid:29574784.

25. Otsuka K, Wayman CM. Shape memory materials. Cambridge Univ Press. Cambridge; 1998.

26. Alcalde MP, Duarte MAH, Bramante CM, de Vasconselos BC, Tanomaru-Filho M, Guerreiro-Tanomaru JM, et al. Cyclic fatigue and torsional strength of three different thermally treated reciprocating nickel-titanium instruments. Clin Oral Investig. 2018;22(4):1865-71. http://dx.doi.org/10.1007/s00784-017-2295-8. PMid:29224061.

27. Goo H-J, Kwak SW, Ha J-H, Pedullà E, Kim HC. Mechanical properties of various heat-treated nickel-titanium rotary instruments. J Endod. 2017;43(11):1872-7. http://dx.doi.org/10.1016/j.joen.2017.05.025. PMid:28951028.

28. Keskin C, Inan U, Demiral M, Keleş A. Cyclic fatigue resistance of reciproc blue, reciproc, and waveone gold reciprocating instruments. J Endod. 2017;43(8):1360-3. http://dx.doi.org/10.1016/j.joen.2017.03.036. PMid:28662877.

29. Silva JD, Martins SC, Lopes NIA, Resende PD, Santos LA, Buono VTL. Effects of aging treatments on the fatigue resistance of superelastic NiTi wires. Mater Sci Eng A. 2019;756:54-60. http://dx.doi.org/10.1016/j.msea.2019.04.037.

30. Auricchio F, Petrini L. A three-dimensional model describing stress-temperature induced solid phase transformations: solution algorithm and boundary value problems. Int J Numer Methods Eng. 2004;61(6):807-36. http://dx.doi.org/10.1002/nme.1086.

31. International Organization for Standardization. ISO 3630-1, Dental Root Canal Instruments—Part 1: Files, Reamers, Barbed Broaches, Rasps, Paste Carriers, Explorers and Cotton Broaches. Switzerland: ISO; 1992.

32. Çapar ID, Arslan H. A review of instrumentation kinematics of engine-driven nickel-titanium instruments. Int Endod J. 2016;49(2):119-35. http://dx.doi.org/10.1111/iej.12432. PMid:25630977.

33. Hieawy A, Haapasalo M, Zhou H, Wang ZJ, Shen Y. Phase transformation behavior and resistance to bending and cyclic

fatigue of ProTaper gold and ProTaper Universal instruments. J Endod. 2015;41(7):1134-8. http://dx.doi.org/10.1016/j.joen.2015.02.030. PMid:25841955.

34. Kim HC, Kwak SW, Cheung GSP, Ko DH, Chung SM, Lee W. Cyclic fatigue and torsional resistance of two new nickel-titanium instruments used in reciprocation motion: reciproc versus waveOne. J Endod. 2012;38(4):541-4. http://dx.doi.org/10.1016/j.joen.2011.11.014. PMid:22414846.

35. Baek SH, Lee CJ, Versluis A, Kim BM, Lee W, Kim HC. Comparison of torsional stiffness of nickel-titanium rotary files with different geometric characteristics. J Endod. 2011;37(9):1283-6. http://dx.doi.org/10.1016/j.joen.2011.05.032. PMid:21846549.

36. Otsuka K, Ren X. Physical metallurgy of Ti–Ni-based shape memory alloys. Prog Mater Sci. 2005;50(5):511-678. http://dx.doi.org/10.1016/j.pmatsci.2004.10.001.

37. Zhang EW, Cheung GSP, Zheng YF. Influence of cross-sectional design and dimension on mechanical behavior of nickel-titanium instruments under torsion and bending: a numerical analysis. J Endod. 2010;36(8):1394-8. http://dx.doi.org/10.1016/j.joen.2010.04.017. PMid:20647104.

38. He R, Ni J. Design improvement and failure reduction of endodontic files through finite element analysis: application to V-taper file designs. J Endod. 2010;36(9):1552-7. http://dx.doi.org/10.1016/j.joen.2010.06.002. PMid:20728726.

39. Viana ACD, Bahia MGDA, Buono VTL. Comparison between the flexibility of three different types of rotary NiTi endodontic instruments. Mater Sci Forum. 2010;643:61-8. http://dx.doi.org/10.4028/www.scientific.net/MSF.643.61.

40. Braga LC, Magalhães RRS, Nakagawa RKL, Puente CG, Buono VT, Bahia MG. Physical and mechanical properties of twisted or ground nickel-titanium instruments. Int Endod J. 2013;46(5):458-65. http://dx.doi.org/10.1111/iej.12011. PMid:23078183.

41. Capar ID, Ertas H, Ok E, Arslan H, Ertas ET. Comparative study of different novel nickel-titanium rotary systems for root canal preparation in severely curved root canals. J Endod. 2014;40(6):852-6. http://dx.doi.org/10.1016/j.joen.2013.10.010. PMid:24862716.

42. Elnaghy AM. Cyclic fatigue resistance of ProTaper Next nickel-titanium rotary files. Int Endod J. 2014;47(11):1034-9. http://dx.doi.org/10.1111/iej.12244. PMid:24392730.

43. Pérez-Higueras JJ, Arias A, de la Macorra JC, Peters OA. Differences in cyclic fatigue resistance between ProTaper Next and ProTaper Universal instruments at different levels. J Endod. 2014;40(9):1477-81. http://dx.doi.org/10.1016/j.joen.2014.02.025. PMid:25146037.

44. Urbina C, De la Flor S, Ferrando F. Effect of thermal cycling on the thermomechanical behaviour of NiTi shape memory alloys. Mater Sci Eng A. 2009;501(1-2):197-206. http://dx.doi.org/10.1016/j.msea.2008.10.026.

45. Galal M. Metallurgical effect on the mechanical behavior of rotary endodontic files using finite element analysis. Bull Natl Res Cent. 2019;43(125):1-5. http://dx.doi.org/10.1186/s42269-019-0168-9.

46. Vieira EP, França EC, Martins RC, Buono VT, Bahia MG. Influence of multiple clinical use on fatigue resistance of ProTaper rotary nickel-titanium instruments. Int Endod J. 2008;41(2):163-72. PMid:18005043.